ANL-6672

ANL-6672

Argonne National Laboratory

REACTOR DEVELOPMENT PROGRAM

PROGRESS REPORT

December 1962

ANL-6672
Reactor Technology
(TID-4500, 18th Ed.)
AEC Research and
Development Report

ARGONNE NATIONAL LABORATORY
9700 South Cass Avenue
Argonne, Illinois

REACTOR DEVELOPMENT PROGRAM PROGRESS REPORT

December 1962

Albert V. Crewe, Laboratory Director

Division	Director
Chemical Engineering	S. Lawroski
Idaho	M. Novick
Metallurgy	F. G. Foote
Reactor Engineering	B. I. Spinrad
Remote Control	R. C. Goertz

Report coordinated by
R. M. Adams and A. Glassner

Issued January 15, 1963

Operated by The University of Chicago
under
Contract W-31-109-eng-38
with the
U. S. Atomic Energy Commission

FOREWORD

The Reactor Development Program Progress Report, issued monthly, is intended to be a means of reporting those items of significant technical progress which have occurred in both the specific reactor projects and the general engineering research and development programs. The report is organized in a way which, it is hoped, gives the clearest, most logical over-all view of progress. The budget classification is followed only in broad outline, and no attempt is made to report separately on each sub-activity number. Further, since the intent is to report only items of significant progress, not all activities are reported each month. In order to issue this report as soon as possible after the end of the month editorial work must necessarily be limited. Also, since this is an informal progress report, the results and data presented should be understood to be preliminary and subject to change unless otherwise stated.

The issuance of these reports is not intended to constitute publication in any sense of the word. Final results either will be submitted for publication in regular professional journals or will be published in the form of ANL topical reports.

The last six reports issued in this series are:

June 1962	ANL-6580
July 1962	ANL-6597
August 1962	ANL-6610
September 1962	ANL-6619
October 1962	ANL-6635
November 1962	ANL-6658

TABLE OF CONTENTS

TABLE OF CONTENTS

TABLE OF CONTENTS

I. WATER-COOLED REACTORS

A. EBWR

The current experimental program established for the EBWR reactor has been successfully completed. The reactor achieved the design objective of 100-Mwt power output and was shut down on December 6, 1962.

The results of the program are being analyzed and will be subsequently issued as a topical report. In the interim, the results will be given periodically as they are obtained.

B. BORAX-V

1. Operations and Experiments

a. Reactor Operations. Zero-power experiments have been completed at conditions up to 600 psig, 489°F with the revised (B-2) boiling core in BORAX-V. The reactor has been brought to pressure with nuclear heat, and the low-pressure steam safety valves have been tested and adjusted.

The reactor and turbine plants were prepared for power operation and were operated at powers up to approximately 5 Mwt to test the steam and turbogenerator systems. On the whole, the first power run was uneventful. The reactor appeared to be very stable at powers up to 5 Mwt, as determined from the linear power instruments.

With the reactor shut down, tests were made to determine the feasibility of operating the boron-addition system at low temperature. Times required for the boron tank to reach reactor pressure after the steam balance valve was opened were 10, 8, and 5 min at 100, 250, and 600 psi, respectively. None of the water hammer, which was experienced in earlier tests with no delay times, was observed. Total time to dump a water-without-boron tank charge to the reactor vessel, including the pressurizing delay time, averaged about 20 min.

Specimens of several materials for use in the steam system have been installed in both the high-pressure steam main and low-pressure casing of the steam turbine to monitor deposition rates of radioactive materials.

b. Reactor Physics. Zero-power critical experiments and control rod calibrations were completed with the BORAX-V boiling core B-2 for operating temperature (489°F, 600 psig) and room-temperature conditions. With the increase of water-fuel ratio in core B-2, the control rod reactivity worths at operating temperature are now slightly higher than the worths at

room temperature. The available excess reactivity of the B-2 core at operating temperature was found to exceed that of the B-1 core by a factor of about two. Integration of the differential control rod worth curves yielded excess reactivity estimates of 11.4% for the core at room temperature and 6.2% for the core at operating temperature. At a power of 5 Mwt, excess reactivity available was about 3.5%, as estimated from the curve at operating temperature.

c. In-vessel Instrumentation. Brief periods of reactor operation were used to obtain data from in-vessel instruments at powers up to approximately 5 Mwt. Information obtained so far includes the intercalibration of all in-vessel thermocouples during hot (489°F, 600 psig) zero-power operation; intercalibration of a miniature flux-mapping chamber against the reactor linear flux recorder; measurement of central boiling-fuel-rod temperatures; and measurement of reactor vessel specimen temperatures.

Thermocouple intercalibration has been difficult because of the lack of true isothermal conditions in the reactor at operating temperature and pressure. At temperatures below 200°F, all water and steam thermocouples agree to within ±1°F; at temperatures near 489°F, the readings of the in-core water thermocouples cover a 20° band, while the downcomer thermocouples cover a 2° band. Readings appear to be reproducible, so it is planned to use relative readings to determine temperature rise during power operation. Addition of control rod seal water as well as operation of the auxiliary circulating pump have shown a major effect on in-vessel water-temperature readings. Indications read from the downcomer thermopiles are influenced so drastically by these factors that differential temperatures have thus far had no meaning.

Data from the fuel rod central thermocouples agree reasonably well with design predictions. They indicate an approximate maximum temperature near the center of fuel assembly position 46 (see Figure 1, p. 4, ANL-6658, Progress Report for November 1962) of 890°F at 5 Mwt.

Because of low coolant velocities, operation of the fuel assembly and downcomer flowmeters has not yet been evident, although the electrical portions of the meters appear to be correct.

Detailed design has been started on a drive for an ultrasonic water-level-sensing device.

d. Water Chemistry. Chemical monitoring of the reactor water during operating periods was begun this month. Continuous resistivity, pH, and chloride analyses were maintained, with intermittent 24-hr analyses of suspended solids. The fission product monitor also operated continuously.

Except for one period discussed below, the resistivity of the reactor water remained better than 1 megohm-cm, chloride ion content remained undetectably low (probably less than 0.02 ppm), and the pH varied between 6.8 and 7.2. Background readings were given by the fission product monitor. Analyses for suspended solids showed a concentration ranging from 0.12 to 0.27 ppm by weight of ignited oxides. Tentatively, these oxides are iron, nickel, aluminum, and chromium, with traces of others. The predominant oxide is Fe_2O_3.

During the 5-Mwt power run, the pH of reactor water dropped to 6.5, resistivity dropped to approximately 470,000 ohm-cm, and the chloride concentration increased from undetectable to 0.3 ppm. Due to the press of operating experiments, the demineralizer could not be used continuously until six days later, at which time the reactor water was cleaned up to a conductivity reading of 2 megohm-cm.

The source of this chloride is unknown. A check on feedwater, which indicated excellent quality, points to the possibility that the chloride may have been in the reactor system deposits and was released in soluble form to the water as power was increased. The lower pH probably resulted from formation of nitric acid.

e. Reactor Transfer Function. The reactor zero-power transfer function ($\delta n/n_0 \delta k$) for core B-2 was measured by both the cross-correlation and null-balance methods at various frequencies between 0.05 and 20.0 cycles/sec. The reactor conditions for the cross-correlation experiment were as follows: 489°F, 600 psig (sat), and ~2 kw. For the null-balance experiment, the reactor conditions were 489°F, 600 psig (sat), and ~10 kw. (The higher power level gave better results with null balance, due to reduction in ion chamber noise.)

Comparison of the phase data of the BORAX-V zero-power transfer function calculated by an IBM-704 (6-group, $\beta = 0.0071$, $\ell = 2.7 \times 10^{-5}$ sec) from data measured by the cross correlation method is very good (within 0.5° in the range from 0.05 to 0.7 cps). The phase results obtained from the null-balance method are also very good at the low frequencies (within 0.1° in the range from 0.3 to 4.0 cps), but the discrepancy is ~5° at the higher frequencies. The gain results for the cross-correlation method are in fair agreement with the calculated gain (within 5%), whereas the null-balance gain results agree very well (within 2%).

Causes for the above discrepancies are presently being investigated.

A simplified dynamic model of BORAX-V at 20 Mwt has been simulated on the 10-amplifier Donner computer, and a resonance is indicated at ~2.5 cps. Transfer function calculations of a more elaborate model are still proceeding on the IBM-704.

Calculations are proceeding on the IBM-1620 computer to determine the steady-state relationship between average void fraction, power level, steam carryunder and carryover on BORAX-V.

2. Preliminary Results of Critical Experiments with Superheater Fuel

A brief investigation of some of the nuclear characteristics of the BORAX-V superheater fuel elements was completed last September. Treatment of the foil-activation data, now nearing completion, has yielded the following information regarding the power distribution within the central superheater zone.

Midplane flux plots indicate only a slight curvature in the radial direction within the superheater zone. Epicadmium uranium fission distribution dropped less than 7% below the central value at any point in the superheater. The ripple at the interface of superheater and boiling zone fuel was sufficient to equal the central value.

Flux shapes in the insulated (rectangular) fuel elements were consistent with the separability assumption. Traverses from edge to edge of fuel plates had similar shapes whether taken in a voided element or at its boundary. The curves were fitted by the equation

$$F(x) = L \exp(-xC) + \exp C(x - W) \quad ,$$

where $F(x)$ was the relative fission rate at a distance x from one edge of the fuel plate and W was the width (9.2 cm) of the fuel plate. Typical fitted values were $L = 0.842$ and $C = 0.182$, giving an effective average of about 82% of the surface activity. In the direction normal to the fuel plates the inner pair received about 5% less flux, effectively, than the outer pair.

3. Modification and Maintenance

The air-ejector exhaust system has been modified to reduce the hydrogen-oxygen explosion hazard by providing for dilution of the gases farther upstream in the system. The 10-cfm air-ejector exhaust rotameter was moved just downstream of the aftercooler and demister. The 4-in. dilution air injection point was moved to a location just ahead of both the "absolute" and activated charcoal filters.

Recordings were made of selected control-rod-drive motor currents during starting and running conditions to determine the effectiveness of reducing motor failures by replacing intermediate-group rod-drive motor rotors with high-starting torque-type rotors. Testing showed the high-torque rotor was no improvement in reducing starting current.

4. Procurement and Fabrication

a. Superheater Fuel. Welding assembly of the third and final instrumented central superheater fuel assembly is nearing completion. Seventeen standard peripheral superheater welded subassemblies have been completed.

b. Experimental Components. Repair and fabrication work on instrumented boiling fuel assembly I-1 was completed. Thermocouples and flowmeter coils checked satisfactorily. The pressure seal plug for instrument leads passed a 900-psi hydrostatic test.

All material specimens for a reactivity worth test of control materials are on hand. These samples are:

(1) 50 w/o boral canned in type 304 stainless steel;

(2) hafnium;

(3) 2 w/o natural boron-stainless steel;

(4) 2 w/o, 93% enriched boron-stainless steel; and

(5) cadmium.

To allow insertion of these specimens in the reactor, a standard boiling fuel assembly has been modified by the deletion of a row of seven fuel rods adjacent to one side and the installation of an aluminum flow baffle, thus leaving a water-filled channel $\frac{7}{16}$ in. thick by $3\frac{3}{4}$ in. wide. An aluminum specimen holder has been designed and is being fabricated.

A new flux wire material, made of gold-5% iron, has been fabricated by the Metallurgy Division. This material is stronger and stiffer than the gold wire formerly used for flux mapping at low powers and should withstand the high-temperature service and stress of insertion and removal from the long in-core pressure thimbles. The fuel rod gamma scanner has been modified to do gamma-counting of continuous flux wires.

Modification was started on an existing counter drive mechanism for the miniature ionization chambers which will be operated in the $\frac{3}{8}$-in. pressure thimbles in the reactor vessel.

A 146-in. Acme threaded stainless steel probe was built for the ultrasonic water-level-measuring device and has been shipped to the vendor for assembly with the sensor.

c. Plant Components. The new air-motor-driven hydrostatic test pump has been received. This higher-capacity pump will permit more dependable testing of the reactor vessel and attendant piping at the hydrotest pressure of 900 psig.

The major parts of the depleted uranium fuel-handling coffin have been made, and only assembly remains. A spare boiling fuel assembly grappler was completed and checked out. Fabrication of the head-on fuel handling tool has been started.

5. Advanced Superheater Fuel

a. Design. Two fuel assembly configurations have been tentatively chosen for continued studies of advanced superheater fuel concepts. The first consists of an annular square array of 4008, $\frac{3}{8}$-in.-diameter, stainless steel-clad UO_2 spheres inside a 3-in. (inside dimension) double-walled square tube and outside a $1\frac{1}{8}$-in. (outside dimension) double-walled square tube, with moderator water surrounding the assembly and in the center tube. The second configuration is a "pea-in-a-pod" design consisting of 72 pods. Each 0.010-in.-thick stainless steel pod cladding tube is formed around 70 spherical UO_2 balls in a row. The OD of the pod is 0.341 in., and there are 5040 UO_2 balls per assembly. The pods are arrayed in a $3\frac{9}{16}$-in. (inside dimension across flats) hexagonal, double-walled tube with a $1\frac{13}{32}$-in. (outside dimension across flats) hexagonal center, double-walled tube. Moderator water is again inside and outside the tubes. The space between the double walls is static-steam-filled and serves as thermal insulation.

b. Development and Testing. Preliminary machine and manual welding tests have been made with joints constructed of Type 406-to-Type 406 stainless steel and with Type 406-to-Type 304 stainless steel sheet 0.045 in. thick. The Type 406 stainless steel material became embrittled in the heat-affected zone adjacent to weld joints, apparently from the growth of large-size grains.

Attempts to draw hemispherical cladding sections of 0.010-in.-thick Type 406 stainless steel have thus far been unsuccessful, due to cold work embrittlement. The die design is now being modified and an intermediate anneal is planned.

An investigation of production techniques for both electrically heated pressure welding and electron-beam welding of hemispherical cladding sections around spherical pellets has started.

Development work on forming a "pea-in-a-pod"-type superheater fuel element (see above) has started. The first attempt to form a 0.010-in.-thick Type 304 stainless steel tube over a row of spherical pellets was only partially successful. Evacuating the inside of the tube heated to 2125°F and slowly pressurizing the exterior with argon to 300 psi resulted in the cladding assuming a spherical shape around part of the pellets, with a cruciform wrinkle between pellets.

II. LIQUID-METAL-COOLED REACTORS

A. General Research and Development

1. ZPR-III

The program of experiments with Assembly 41, a 440-liter core with a 5 to 1 U^{238}:U^{235} ratio, was completed during this month. Among the final experiments were measurements of enriched boron carbide worth per column in a low-density radial blanket, a foil irradiation for a fine axial flux distribution, and extensive measurements of Rossi-alpha.

a. Worth of B_4C Rotary Control Rod in Low-density Radial Blanket. At the conclusion of radial blanket experiments involving EBR-II type blankets, the worth of enriched boron carbide per axial column was measured in a low-density radial blanket at $\frac{1}{2}$ in. from the core and again at 6 in. from the core. The blanket region in which the measurements were made was a 30° wedge sector around the core in both machine halves, containing about 21 v/o depleted uranium, 21 v/o graphite, 30 v/o sodium, and 20 v/o steel. This experiment was part of an evaluation of a rotary control rod scheme in this low-density type of blanket. A similar experiment was performed previously in the regular high-density radial blanket of the assembly with about 84 v/o depleted uranium and 9 v/o steel. A comparison of the "rod" worth in the two blanket compositions is given in Table I. It is seen that the overall reactivity variation during "rod" rotation is about the same in both blankets, but that a larger radius of rotation in the low-density blanket could provide additional worth.

Table I. Mockup Rotary B_4C Control Rod Experiment

Radial Position of 2 x $\frac{1}{2}$ x 16-in. Column	Worth (inhours) of Enriched B_4C[a] (0.518 kg[b]) Replacing Blanket Material	
	In High-density Blanket	In Low-density Blanket
$\frac{1}{2}$ in. from core	-39.0	-44.6
6 in. from core	- 2.4	- 6.6

[a]Enriched B_4C (which is 69.3 w/o boron) contains 90.7 a/o B^{10}.
[b]Equivalent to 20.3 g B^{10}/in. of axial length.

b. Foil Irradiation for Fine Axial Flux Distribution. During axial traverse experiments with uranium fission counters and $B^{10}F_3$ proportional counters, count rates appeared to dip as the counters were passed through the midplane of the reactor. It was thought that this effect could be due to flux depression at the interfaces where the drawer fronts interrupt the

continuity of the enriched uranium fuel columns. An irradiation was therefore made of enriched uranium foils placed at regular axial intervals along the top of drawer 1-P-16 to determine if this flux depression was evident by this method. Activation of these foils was then determined with scintillation detectors. No depression of relative activation was observed for the foils irradiated near the core midplane at least within an observed accuracy of 0.8%.

c. Source Worth Experiment. Prior to experiments for measuring Rossi-alpha by means of the ZPR-III startup sources, a measurement was made of these sources when "in" at about 4 in. from the core radial edge. The difference in critical position at 20 w with the source "in" and "out" amounted to less than 0.2 inhour.

d. Rossi-alpha Measurements. Extensive measurements of Rossi-alpha, involving variations of the usual procedures, were made with Assembly 41. Two methods were employed to obtain subcriticality: in one control and/or safety rods were withdrawn, and in the other the average core fuel density was decreased. Higher degrees of subcriticality were also used, substantial count rates being provided by use of the startup sources moved closer to the core.

The preliminary average value of α at delayed critical derived from the data is -5.55×10^{4} sec^{-1}. With $\alpha = -\beta/\ell$, and $\beta = 0.0073$, the neutron lifetime is then 13.2×10^{-8} sec.

e. Worth of Thorium at Core Edge. A reactivity coefficient measurement was made for thorium at the core radial edge near the midplane. Thorium samples, 2 x 2 x 1 in. in size, were substituted for void at the front of 1-J-12 and 2-V-20. Thorium was found to be worth -0.2 inhour/kg at that position.

2. Preparations for ZPR-VI and ZPR-IX Operation

a. ZPR-VI. The ZPR-VI facility has been thoroughly checked out and is ready for operation. A pre-operational inspection survey has been performed by personnel of the Chicago Operations Office.

The installation of the argon purge system has been completed and is being tested.

The aluminum housings used to cover the drive springs on the safety rod drive mechanism showed wear due to contact between the housing and the springs. One aluminum housing was replaced with one made of stainless steel and was satisfactorily tested. As a result, other safety rod drive mechanisms on the facility are being similarly modified.

b. ZPR-IX. The Laboratory shops are continuing to rework the aluminum tubes for the matrix. Approximately 15% of the tubes have been reworked and are ready for assembly into 5-by-5 bundles.

c. Miscellaneous. Shop work on the mechanical oscillator for use in the Doppler measurement experiments is approximately 75% complete.

3. AFSR

The early part of the month was devoted to making further measurements with the reactivity meter, and modifications to the equipment were made based on experience to date. One change which will be tried is use of a logarithmic amplifier to avoid range-changing and to reduce problems of time response.

Work is delayed on the color discriminator for detection of neutrons in the presence of gamma radiation. The three replacement crystals for those damaged earlier in shipment arrived; only the CsI crystal was usable - the NaI and LiI crystals were again damaged in transit, possibly by low temperatures in shipment or warehousing.

The reactor was operated to obtain more information on two of the RED solid-state neutron spectrometers, and foils were irradiated to calibrate instruments for measurements of EBR-I breeding gain.

A new gamma-monitoring system has been installed, tested, and calibrated. Its advantage is that it is a much simpler checkout system, which is being incorporated into a new version of the weekly checkout sheets. The operating manual is being revised to include this and other changes that have occurred since the manual was originally issued in 1960.

B. EBR-I

1. Calibration of Outer Uranium Blanket

Having achieved initial criticality with the reactor, subcritical measurements were made to determine the worth of the uranium outer blanket (outer cup) over its full length of travel. The method used for calibrating the cup over the range from 80 to 5 in. is identical to that described by Kirn in ANL-6392, and it also serves as a check in the region from 5 to 0 in. Methods and results applicable to these two regions are described below.

Two detectors were used to measure the neutron flux. One, designated as Channel 2, consisted of a gas-flow fission counter located at midplane in hex L. The other, designated as Channel A, consisted of an RCL BF_3 counter located at midplane in hex J. A summary of the subcritical counting results is given in Table II. The data for Channel A

for elevations 80 to 7.5 in. have been normalized for consistency with data from Channel 2 over the same region. This adjustment was considered necessary in view of a number of spurious pulses noted in Channel A at low counting rates. Above 7.5 in., corrections were not considered necessary. Effectively, then, all information from both Channels for elevations between 80 and 7.5 in. is based on Channel 2 data.

Table II. Subcritical Counting Results

Cup Position (in.)	Channel 2 (c/min)	Channel A (c/min)
80	185	618
40	183	611
20	210	702
10	300	1001
7.5	469	1570
6.0	682	2161
5.0	868	3016
4.0	1276	4517
3.0	2138	7303
2.0	4750	15508
1.25	19745	63600

With the reactor subcritical at a cup position of 1.25 in. (critical position 0.98 in.), control rod No. 2 was dropped and a subcritical count was taken with both channels. This procedure was repeated for the following rod removals: control rods 3, 1, and 4. Safety rods were dropped according to the following pairs: 7 and 8, 1 and 2, 3 and 4, and 5 and 6. Finally, the safety plug was also dropped in an attempt to measure its worth.

The subcritical counting data for the two channels corresponding to the various reactivity losses are summarized in Table III. The values given in columns (4) and (5) are simply the respective products of the counting rate (c/min) and the total negative reactivity (Ih) removed from the system, assuming that one control or safety rod is worth 30 Ih (actually a measured value). Disregarding the first entry for both channels, average values of 9.92×10^5 and 3.31×10^6 were found for $n_1 \Delta k_1$ in Channels 2 and A, respectively. The worth of the cup between its "down" position and 1.25 in. may then be found from these constants and the respective counting rates at the "down" position given in Table II.

Hence, for Channel 2,

$$\Delta k_2 = n_1 \Delta k_1 / n_2 = 9.92 \times 10^5 / 185 = 5360 \text{ Ih} \quad ,$$

and for Channel A

$$\Delta k_2 = 3.31 \times 10^6/618 = 5360 \text{ Ih} \quad .$$

Table III. Subcritical Counting Results for Control-Safety Rod Removal

(1)	(2)	(3)	(4)	(5)
Total No. of Rods Out	Channel 2 (c/min)	Channel A (c/min)	Channel 2 ($n_1\Delta k_1 \times 10^{-5}$)	Channel A ($n_1\Delta k_1 \times 10^{-6}$)
1	29571	95441	8.85	2.86
2	16130	53380	9.68	3.20
3	11066	36390	9.98	3.28
4	8184	27259	9.80	3.27
6	5529	18314	9.95	3.30
8	4139	13950	9.91	3.34
10	3337	10867	10.00	3.14
12	2812	10089	10.10	3.62
Plug	2420	8591		
Average			9.92	3.31

The agreement between the values for the two channels is not surprising, since the "cup-down" data for Channel A are based, in part, on a cross-normalization of data for elevations above 7.5 in. The normalization by itself, however, cannot account for the exact agreement; this must be regarded as fortuitous.

A subsequent cup calibration (through period measurements) between 1.25 and 0.00 in. resulted in a value of 225 Ih for the reactivity worth. Hence, the cup in its entire travel between fully "down" (80 in.) and fully "up" (0.00 in.) amounts to 5360 + 225, or 5585 Ih. Assuming from ANL-6411 (page 62) that 950 Ih = 1% $\Delta k/k$, the equivalent value becomes 5.89% $\Delta k/k$.

The cup worth as a function of elevation between fully "down" and fully "up" is summarized in Table IV. Allowance has been made for the worth between 1.25 and 0.00 in.

A plot of the reactivity worth between the fully "up" and fully "down" positions as a function of elevation is given in Figure 1.

Table IV. Cup Worth As a Function of Elevation

Cup Elevation, in.	Cup Worth - Channel 2		Cup Worth - Channel A	
	Ih	%Δk/k	Ih	%Δk/k
80	5585	5.89	5585	5.89
40	5655	5.95	5655	5.95
20	4955	5.22	4955	5.22
10	3535	3.72	3535	3.72
7.5	2345	2.47	2335	2.46
6.0	1675	1.77	1755	1.85
5.0	1370	1.45	1335	1.41
4.0	1005	1.06	959	1.01
3.0	690	0.73	679	0.72
2.0	434	0.46	439	0.47
1.25	275	0.29	277	0.30
0.00	0	0.00	0	0.00

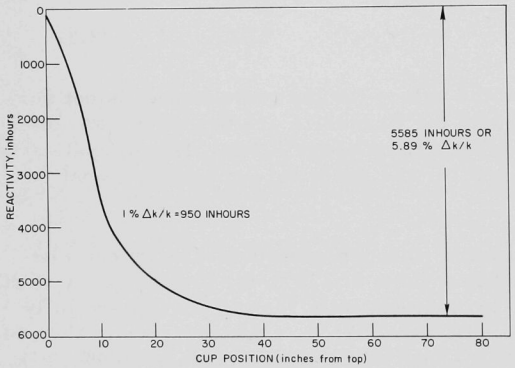

Figure 1

EBR-1, Mark IV Uranium Cup Calibration

An expansion of the same figure in the region from 0 to 5.5 in. is given in Figure 2. From this it may be seen that the worth of the cup over the range from 0 to 5.15 in. is approximately 1440 inhours, or 1.52% Δk/k. Since the cup calibration through period measurements still does not extend to 5.15 in., it is impossible at this time to carry out a direct comparison of the respective 5.15-in. worths. A comparison of values at 4 in., however, can be made. From Figure 2, the worth between 0 and 4 in. is given as 1005 inhours. This compares with a value of 915 inhours obtained through period measurements, as illustrated in Figure 3. Two reasons can be suggested for the discrepancy. One is concerned with the value of 30 inhours assumed for the worth of a control or safety rod. Actually, values ranging from 28 to 32 inhours were measured; the value

30 was assumed to be a reasonable average. Secondly, the subcritical values were based on a somewhat different core loading, namely, with two large "holes" present in the Mark III blanket and with two fewer fuel rods.

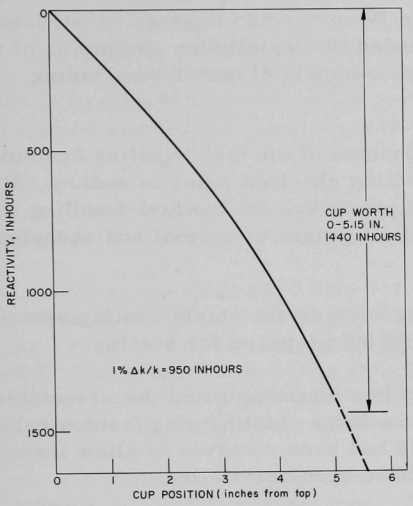

Figure 2. EBR-I, Mark IV Uranium Cup Calibration

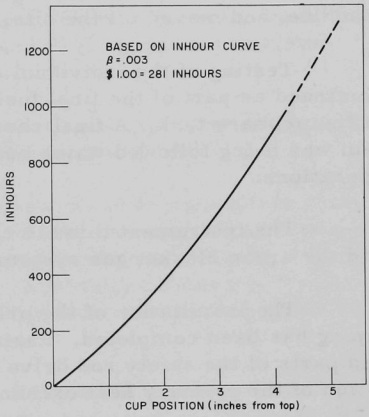

Figure 3. EBR-I, Mark IV Uranium Cup Calibration Curve - Dec. 1962

A rough estimate of the worth of the uranium safety plug can also be made from the data taken. Using the data from Channel 2, the more reliable at low counting rates, a value of 51 inhours or 0.054% $\Delta k/k$ was deduced.

2. Determination of Temperature Coefficient

The isothermal reactor temperature coefficient has been measured as 3 inhours/°C over the range between 30 and 180°C. There is no apparent change in the temperature coefficient with temperature.

3. Adjusted Critical Mass

During the approach to critical, two 1-$\frac{1}{16}$-in.-ID thimbles were installed in two blanket subassemblies for in-core counters. Each thimble replaced seven Mark III blanket rods in the subassembly. With these thimbles now replaced with Mark III blanket rods, the adjusted minimum critical mass is 28 kg total Pu, or 26.4 kg Pu^{239}. This value does not consider the beryllium-antimony source which also replaces seven blanket rods in a subassembly.

C. EBR-II

1. Reactor Plant

During the month, the Package IV contractor finished construction work in the Reactor Plant, which included the installation and piping of the sodium-to-sodium heat exchanger and assembly of the fuel-unloading machine, and moved off the site.

Testing of the individual components of the fuel-handling system continued as part of the final fuel-handling checkout prior to sodium filling of the primary tank. A final checkout procedure for the fuel-handling system was being followed which covered all phases of normal and abnormal operations.

The instrument thimble cooling system, the shield cooling system, and the argon blanket gas system are being prepared for startup.

The installation of the primary heat exchanger and the associated piping has been completed. Parts of the large rotating plug festoon cable and parts of the safety rod drive which had been removed to allow installation of the primary heat exchanger have been reinstalled.

The vendor-supplied Interbuilding Coffin has been received at the EBR-II site. The coffin is undergoing tests for leak tightness and is being inspected for damage. The fabrication at Argonne of component parts for the Fuel Transfer Coffin is continuing. A blower for recirculating the argon coolant is being returned to the manufacturer for examination. ANL tests of the blower revealed that $1\text{-}\frac{1}{4}$ hp was required to drive the blower instead of the $\frac{3}{4}$ hp specified.

2. Power Plant

Activities in the Power Plant have been directed toward preparing the steam system for operation early in the next period. This system will initially use 175-lb building steam to supply heat to the steam generators in the secondary sodium system during vacuum bake-out and sodium filling. Subsequently, during secondary system cold trapping, the steam system will be maintained at temperature and pressure by use of the secondary system electrical heaters. All instruments and system components necessary for these operations are in final phases of testing or already placed in service.

Inspection and reassembly of the startup feedwater pump gear box was completed. Because of undetermined noise during operation, all bearings were replaced, although three of the four originals appeared in perfect condition. The other showed no sign of wear but had minute dents and scratches. A factory representative was not able to pinpoint the noise, but is satisfied that this unit is in good operating condition now.

3. Sodium Boiler Plant

Final preparations and testing were in progress during the period and directed toward sodium filling early next month.

Cleaning, packing, identification, adjustment, and testing of all valves were completed. During checkout of the drain valves, it was noted that one remained closed even after the stem was withdrawn by hand. Investigation showed the stem was not engaged in the gate, and this was corrected.

The location of all points for the determination of pipe movement during heat-up was completed and elevations recorded.

All argon lines were checked for leakage and to insure free flow. Identification of lines, valves, and equipment was accomplished by stenciling. Plant services, such as instrument air and cooling water, were tested. Instrument technicians completed calibration of thermocouples and pressure transducers and checkout of the Panascan portion of the control panel for the secondary sodium system.

Checkout of the relief system was started. A leak was found in the relief tank and repair commenced. Adjustment of hangers continued during the month. Work on the control system for the secondary sodium pump also continued. Replacement of defective heaters on the cold trap was held up pending delivery of new units.

Installation of vacuum equipment for vacuum bake-out of the secondary sodium system was completed.

4. Fuel Cycle Facility

Work being done by the J. F. Pritchard Company, under the Package 4 contract, was concluded this month. This contract provided for the installation of equipment for the EBR-II Fuel Cycle Facility by the Company under the direct supervision of Argonne National Laboratory personnel.

A view of the melt-refining area in the Argon Cell of the EBR-II Fuel Cycle is shown in Figure 4. A melt refining furnace, service feed throughs, manipulator bridge cranes, and shielding window shutters can be seen.

A diesel generator installed on the service floor of the Fuel Cycle Facility will provide emergency power for the operation of essential equipment in this building. In case of an electrical power failure, the electrical load can be automatically transferred to the diesel generator within 5 to 6 seconds. The emergency power system has performed satisfactorily during several recent power failures.

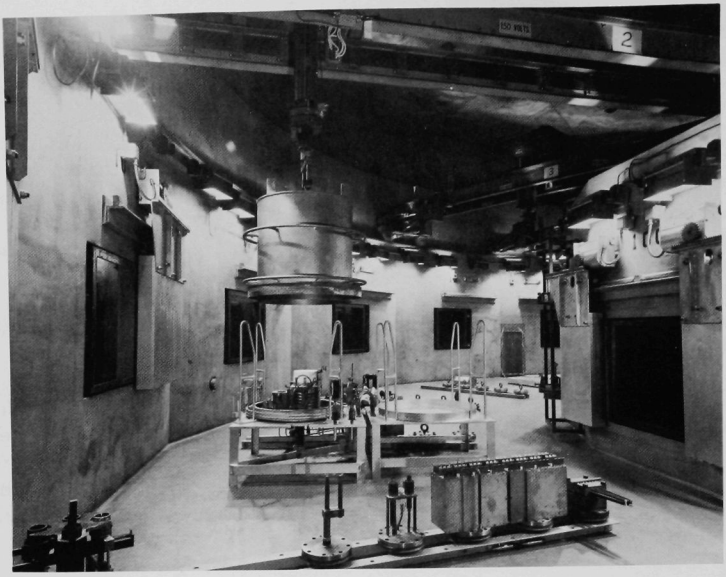

Figure 4. Inside the Argon Cell of EBR-II Fuel Cycle Facility. A melt-refining furnace is shown with its bell jar cover in the "up" position. The installation of the furnace was carried out by remote means. In the right foreground, a bank of service feed throughs is seen at floor level. Shown (from left to right) are induction heating, vacuum, electrical and thermocouple, and pneumatic feed throughs. In the left foreground, a part of a manipulator tool rack and changer is shown. Manipulator bridge cranes span the work area. Two steel shielding shutters to protect the windows from radiation damage when the windows are not in use are seen hanging from the window shutter rails above the shielding windows. A single-type shielding shutter is on the left; a split-type shielding shutter is on the right.

The off-gas monitoring system has been received at the EBR-II site. This system will continuously monitor the total activity in the gas discharged from the off-gas hold-up tank. The hold-up tank stores the gases which are released in melt-refining and in the oxidation step of the skull-reclamation process until meteorological conditions are favorable for the discharge of the gases through a 200-ft-high stack. Drawings for the installation of the off-gas monitoring system are being prepared.

a. Argon and Air Cells. Corrective work is being done on the light luminaires in the Argon Cell and in the Air Cell. Insulating blocks made of Rosite 3250-C (a product of Rostone Corporation, Indiana) will replace the ceramic insulators presently in use. Rosite 3250-C is a hot-molded polyester plastic which is reinforced with glass fibers and which contains a high percentage of mineral fillers. It has excellent gamma-radiation stability and high impact strength.

The first phase of leak testing of the argon cell was begun by closing all penetrations and reducing the internal pressure to 10 in. of water below atmospheric pressure. In a 65-hr test, the differential pressure decreased at a rate corresponding to an inleakage of about 0.12 ± 0.02 cfm, to be compared with the desired maximum inleakage of 0.01 cfm at a differential pressure of 4 to 6 in. The cell was then entered to search for leaks by sound, and by soaping and Freon testing. After repairing several leaks around manipulator openings and the pivot tower, a re-test showed the leak rate to be reduced to 0.045 ± 0.01 cfm. Further checking will be done next month when the cell is filled with nitrogen.

The pressure-control system for the argon cell was tested with heat loads ranging up to 120 kw in the cell. It was found possible to maintain the set pressure within $\pm\frac{1}{4}$ in. of water on cycles of varying duration. At low heat loads, control was more difficult due to the presence of overly large refrigerant expansion valves which will be replaced.

A pair of Model A manipulators was installed in the argon cell, and a periscope was placed in the air cell wall. The mockup area has been equipped with benches for testing and functioning of in-cell equipment components. The decanner was assembled remotely with an electromechanical manipulator. Repairs are being made to correct shielding deficiencies in the air cell transfer lock and door.

b. Fuel Subassembly Dismantler. The prototype Fuel Subassembly Dismantler, being developed to remove the fuel and blanket elements from a subassembly, has been extensively redesigned to improve handling and visibility during operation. The dismantler can be used to disassemble all seven of the core, blanket, control and safety subassemblies used in the EBR-II reactor. Attachments required for other than the fuel subassembly remain to be designed.

All of the operating units forming the dismantler are replaceable and have been designed for ease of assembly, operation and remote repair.

A rotating support has been designed which enables the subassembly to be loaded vertically into the dismantler. Cooling air is drawn through the subassembly into the support by means of a suction cooling system.

The current prototype dismantler will require the use of Model 8 master-slave manipulators equipped with special tongs to remove the fuel elements from the support grid. All of the new units and modifications to a number of existing units forming the dismantler are scheduled for completion by the end of the month.

The semi-automatic device for removing the fuel elements from the support grid, the Fuel Element Removing Machine, is about 80 percent complete in design and fabrication is about 50 percent complete.

The control wiring and air-control valve system for the pneumatic cylinders have been installed in Idaho.

c. Spiral Decanning Machine. The machine has been remotely assembled in the Fuel Cycle Facility at Idaho. Because the argon cell was not accessible, it was installed in the air cell as a trial run by the operating personnel, using only the installation manual for instructions. The installation required about 5 hr.

5. Process Development

a. Melt-refining Process Technology. The use of a chloride flux (calcium chloride containing magnesium fluoride as a rare earth oxidant) in the melt-refining process is being investigated. Although the utility of using the flux for the recovery of uranium in melt refining has been demonstrated, the behavior of plutonium in the flux-liquid metal system needs to be evaluated. Preliminary information suggests that plutonium losses can be kept below one percent.

b. Skull-reclamation Process. Prototype plant-scale process equipment for studying the oxidation of the skull remaining in the crucible after the melt-refining step has been installed in the EBR-II mockup area. Equipment items include the skull-oxide-processing furnace, a unit for the removal of oxygen from the oxidation furnace, and process controls.

Two additional demonstration runs of the skull-reclamation process on a 130-gm uranium scale were completed except for the final process step of retorting. No mechanical difficulties were encountered. However, in the transfer of the zinc phase following the noble metal extraction, stirring of the zinc was shown to be necessary in order to keep noble metal particles in suspension in the metal phase. (The solubilities of the noble metals are exceeded at the temperature, about 525°C, at which the zinc is transferred.)

To learn how completely the uranium in a recycled heel would be oxidized during noble metal extraction, the uranium heel from the reduction step of one run was recycled to the noble metal-extraction step of the next run. The flux used in noble metal extraction consisted of (mole percent): 47.5 $MgCl_2$, 47.5 $CaCl_2$, 5 MgF_2. To this flux, 2 w/o zinc chloride was added as an oxidant. The waste ingot from the noble metal extraction step of the second run contained only 0.0004 percent uranium.

Distillation of magnesium-zinc in the melt-refining furnace is being studied as an alternative to retorting zinc-and-magnesium-coated uranium after the intermetallic decomposition step of the skull-reclamation process. A condenser design is currently being evaluated in which the condensed magnesium-zinc vapors are collected in a collector which will be discarded after each run. The condenser and furnace crucible, however, would be used for more than one run (see Progress Report, November 1962, ANL-6658, page 23). In two recently completed runs, the component parts of the condenser were fabricated of a more impervious grade of graphite (ATJ) than the graphite (CS) used in previous runs. In each run, 1000 gm of 50 w/o magnesium-zinc was distilled from the crucible. In the first run, 92.8 percent of the charge was collected in the collector, 2.2 percent was collected in the condenser, 2.2 percent was collected on the Fiberfrax insulator, and 2.8 percent could not be accounted for. In the second run, 91.2 percent of the charge was collected in the collector, 5.1 percent was collected on the Fiberfrax insulator, and 3.7 percent could not be accounted for. No magnesium-zinc was found in the condenser. A comparison of the results of these tests with previous tests shows that some improvement was obtained by using the more impervious grade of graphite. A greater amount of magnesium-zinc was collected in the collector (91 to 93 percent as compared with 85 percent for the CS graphite) and a lesser amount was found on the Fiberfrax insulator as a result of leakage from the condenser (2 to 5 percent as compared with 8 percent).

c. Plutonium Recovery Process. The solubilities of uranium as a function of calcium concentration up to about 25 w/o calcium in calcium-zinc solutions have been redetermined at 700, 750, and 800°C. The present experiments, in which tantalum filter frits were used for sampling, resulted in higher values for the solubility of uranium than those obtained in previous experiments in which graphite filter frits were used (see ANL-6379, p. 66). The shape of the curve resembles that obtained for the solubility of uranium in the magnesium-zinc system, but the solubility of uranium is lower in the calcium-zinc system, especially at higher calcium concentrations. The results of the experiments are shown in Figure 5.

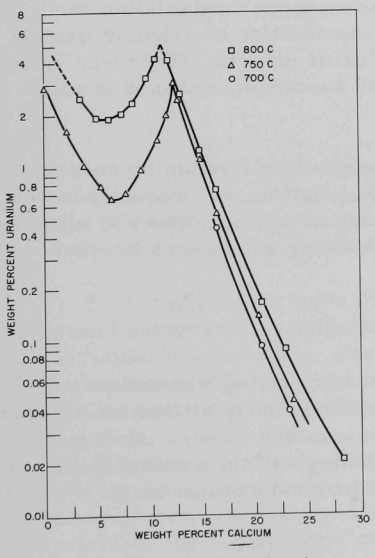

Figure 5. Solubility of Uranium in Calcium-Zinc Solutions

d. Materials and Equipment Evaluation. The stabilities of 0.5 w/o uranium-5 w/o magnesium-zinc solutions at 800°C in a CCT grade (low-ash) graphite crucible, in alumina crucibles containing 0.8 percent silica, and in a high-purity alumina crucible were studied in 24-hr and 48-hr

tests. Unacceptably large decreases in uranium concentration occurred in the graphite crucible. In the silica-alumina crucible, small decreases in uranium concentration occurred, as well as pickups of about 200 ppm aluminum and 500 to 800 ppm silicon. No loss of uranium from solution occurred in the high-purity alumina crucible.

e. Sodium Removal. Irradiated fuel subassemblies on discharge from the EBR-II reactor will be coated with a thin film of sodium. A sodium removal station is to be located in the passageway between the Reactor Building and the Fuel Cycle Facility. A process for the removal of the sodium has been developed which involves the conversion of the sodium to the hydroxide and the removal of the hydroxide by means of a water wash. An equipment layout has been completed. Specifications for equipment items are being prepared.

The possibility of using mercury, rather than steam and water, for the removal of sodium adhering to EBR-II fuel assemblies after they are removed from the reactor has been studied. When a mock stainless steel fuel pin coated with sodium was placed in mercury under a nitrogen atmosphere, the reaction proceeded smoothly with a heat evolution estimated at about 4000 cal/mole, which is one-tenth the value of the heat evolved in the sodium-steam reaction.

f. Analytical Developments. Absorption peaks obtained by spectrophotometric measurements of uranium oxide-molten chloride systems have been attributed to an oxygen-bearing uranium (V) species, probably UO_2Cl. A similar spectrum has been obtained from a petrolatum mull of anhydrous uranium oxytrichloride. On the addition of uranium oxytrichloride to lithium chloride-potassium chloride eutectic, there was some evidence for the characteristic uranium (V) spectrum, although it was poorly defined.

A method for determining technetium in fissium by colorimetry with dithiol, following separation by distillation, was recently tested. These tests showed that redistillation of reagents is necessary to eliminate false results due to the presence of reducing substances in ethyl alcohol and amyl acetate.

6. Training

During December, intensive classroom training was conducted with the goal of completing this phase of training and qualification as soon as possible for those operators who will be involved in early shift work. At that time, the completion of systems training and the gaining of experience leading to operator qualification must be conducted on shift.

A Personnel Protection and Plant Safety course, Fuel Handling Systems and Electrical Systems training sessions, and training in Power Plant Systems for power plant operators were started in December.

D. FARET

1. Selection of Core Material

One of the experimental programs planned for the FARET program is the investigation of the effect of cladding materials on the sodium void coefficient. The structural materials considered were niobium, vanadium, and stainless steel. The niobium and vanadium were chosen for their high strength properties at high temperature (up to 1100°C) and compatibility with lithium, sodium, and UC. The high-temperature strength properties of vanadium are not as good as those of niobium; in fact, the ductility of vanadium alloy is reported as poor. However, its low capture cross section, being of the same order of magnitude as that of stainless steel, makes vanadium attractive with respect to neutron economy. The preliminary results of the calculations for sodium void coefficient for a variety of compositions are given in Table V.

Table V. Effect of Core Structural Material on the Sodium Void Coefficient

Core Sizes, liters	Length-to-diameter Ratios	Composition, Vol-% of Pu-UC/Na/Structural Material	Sodium Void Coefficient ($\times 10^6$) (Equivalent Spherical Geometry)		
			Niobium	Vanadium	Stainless Steel
3000	1.00	25/59/16	+8.9	+7.4	~+4.4
3000	0.25	25/59/16	+5.3	+3.3	+0.42
400	1.00	30/52/18	-1.1	-	-3.75
400	0.25	30/52/18	-2.7	-	-5.6
50	1.00	25/59/16	-6.7	-8.4	-7.6
50	0.25	25/59/16	-6.7	-8.4	-7.6
50	1.00	50/25/25	-1.94	-2.7	-2.6
50	0.25	50/25/25	-2.2	-2.9	-2.8

The calculations were made for spherical geometry having the enrichments computed for cylindrical geometries with length-to-diameter (L/D) ratios of 1 and 0.25. The results indicate that the effect of vanadium on the void coefficient is only slightly better than that of niobium, even though its capture cross section is much lower.

It appears that the spectral effects of vanadium are similar to those of niobium. A more detailed analysis is planned to investigate the competition between capture, spectral, and leakage effects of these structural materials on the sodium void coefficient.

2. Doppler Measurements

In ANL-6597 (Progress Report for July, 1962, p. 23), a preliminary design of a thermally insulated, ceramic pellet-type fuel element for making in-pile Doppler coefficient measurements in the FARET reactor was described. The objective in the design of the element was to permit the fuel temperature to be changed without changing the clad temperature or the overall fuel length significantly. Additional development work on the design of the experimental equipment and program is in progress.

Fuel temperatures may be changed without changing reactor power or coolant flow by varying the gas composition and pressure, and hence the thermal conductivity in the gap between pellets and cladding, or by changing reactor power and coolant flow rates. The gas in the gap is either helium or argon at a pressure of either 760 or $<10^{-3}$ mm Hg.

Table VI shows, for a 0.020-in. gap, the range of reactor fuel temperature changes calculated to result from changing conditions of the gas in the gap in the zoned core loading. Experimental measurements will be made to verify the validity of the calculations. Large fuel temperature changes can also be obtained by changing the reactor power and coolant flow rate to maintain constant cladding and coolant temperatures.

Table VI. Calculated Conditions for FARET Zoned Core Loading

Average Coolant Temperature (°C)	Initial Reactor Power (Mwt)	Final Reactor Power (Mwt)	Initial Gas in 0.020-in. Gap	Final Gas in 0.020-in. Gap	Maximum Fuel Surface Temperature Increase (°C)	Maximum Cladding Temperature Increase (°C)
593	10	10 (no change)	Helium at 760 mm Hg	Argon at 760 mm Hg	327	0
593	10	10 (no change)	Helium at 760 mm Hg	Helium at $<10^{-3}$ mm Hg	505	0
593	2.5	10	Argon at $<10^{-3}$ mm Hg	Argon at $<10^{-3}$ mm Hg (no change)	397	10
427	2.5	10	Argon at $<10^{-3}$ mm Hg	Argon at $<10^{-3}$ mm Hg (no change)	444	10
593	2.5	10	Argon at 760 mm Hg	Argon at 760 mm Hg (no change)	336	10

The first two items in Table VI illustrate the gap conduction control method, and the last three items illustrate the reactor power coolant-flow control method.

The current appearance of the fuel element, in the form of a model for out-of-pile development work, is shown in Figure 6. The model fuel pellets have four axial holes, one through the center and the other three equally spaced on a radius. The inner hole is to provide access for an electrical resistance heater to be used to simulate nuclear heating. The

other holes are for thermocouples; in other words, it will be possible to install three thermocouples in the model pellets. The prototype (in-pile) pellets are to have only one hole, axial at the center, for thermocouple installation.

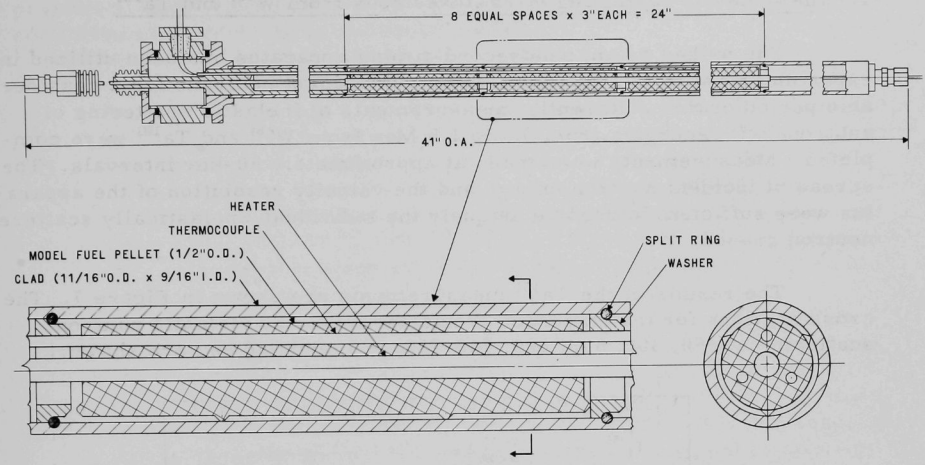

Figure 6. FARET Model Fuel Element for Out-of-pile Tests

The model element is to be used for measurement of gap conductances and for development of pellet-support devices, thermocouples, fuel pellets, and gap-gas-control equipment. A platinum heater, consisting of a 0.006-in.-wall split tube, for the model element has operated satisfactorily at temperatures up to 1700°C in air.

III. GENERAL REACTOR TECHNOLOGY

A. Applied Reactor Physics

1. The Inelastic Scattering of Fast Neutrons from W^{184} and Ta^{181}

The pulsed beam, nanosecond-timing apparatus has been utilized in experimental studies of inelastic scattering of fast neutrons for a considerable period of time. Recently, measurements of inelastic scattering of neutrons with energies from 0.3 to 1.5 Mev from W^{184} and Ta^{181} were completed. Measurements were made at approximately 50-kev intervals. The spread of incident neutron energy and the velocity resolution of the apparatus were sufficient to resolve uniquely the individual, inelastically scattered neutron groups.

The results of the Ta^{181} measurements are shown in Figure 7. The cross sections for the excitation of nuclear levels by inelastic neutron scattering at 150, 300, 500, 620, 700-780, 900, and 980 kev are shown.

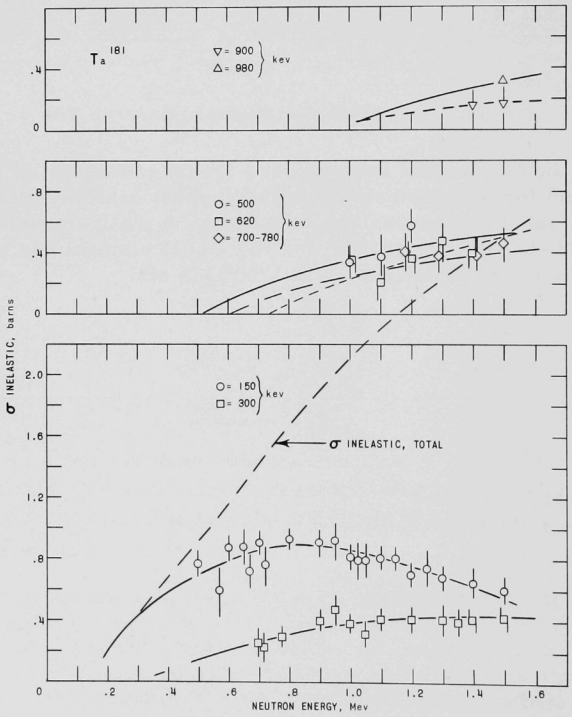

Figure 7. The Inelastic Scattering Cross Section of Ta^{181}

Figure 8 gives a similar set of cross sections resulting from the inelastic scattering of fast neutrons from W^{184}. Scattering to residual nuclear levels in W^{184} at 111, 365, 690, 900, 1000, and 1120 kev was observed. It is evident from the inelastically scattered neutron groups that the inelastic scattering process at these energies in both tantalum and tungsten is governed by the collective motions of these deformed nuclei.

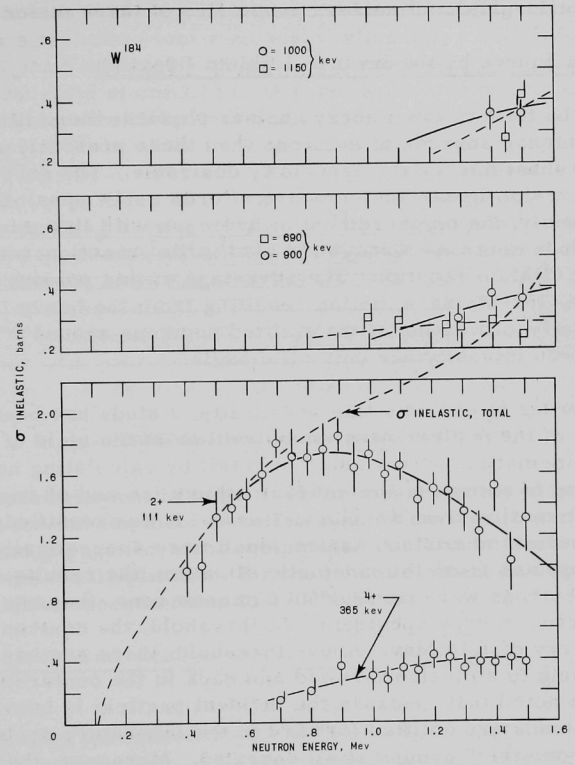

Figure 8. The Inelastic Scattering Cross Section of W^{184}

Theoretical calculations with the objective of interpreting such processes have been initiated. In principle such interpretations are a straightforward application of the nuclear optical model. In practice, they are greatly complicated by the nonspherical nature of the requisite nuclear potential.

The total inelastic scattering cross section can be obtained directly from the individual excitation functions and is indicated on the above figures. In all measured instances, both the total inelastic and partial inelastic cross sections were found to be isotropic. This isotropy simplifies the application of the measurements to reactor theory, but raises some questions dealing with the theory of such reactions. The knowledge of inelastic scattering from Ta^{181} and W^{184} is particularly pertinent to certain reactor concepts due to the unique metallurgical and nuclear properties of these materials.

2. Neutron Source by the Inverse Lithium Reaction

In the field of low-energy nuclear physics, there is a continuing need for more intense sources of neutrons than those presently available. Sources which give short bursts are especially desirable. The development of high-energy heavy-ion linear accelerators affords a new possibility for such a source, namely, the bombardment of hydrogen with lithium-7 ions. This would produce neutrons through the $p(Li^7,n)Be^7$ reaction, which can be called the inverse lithium reaction. The advantage of this possibility would be that the large center-of-mass motion resulting from the heavy incident particle produces self-collimation of the emitted neutrons around 0°. The result is a high neutron intensity per unit solid angle.

In order to evaluate this possibility, a study has been made of the kinematics of the nuclear reaction as well as of the yield of a practical target. The kinematics were studied in detail by calculating neutron energies as a function of energy of the incident lithium ion and of angle of emissions. The 704 kinematics code RE 222 was used. It was modified so as not to give incorrect results at neutron angles which were energetically impossible. As could be expected from the kinematic situation, the results showed that, while the neutrons were confined to a narrow cone, they are also limited to a fairly narrow energy spectrum. At threshold, the neutrons are emitted with an energy of 1.44 Mev. Above threshold, there are two energy groups, corresponding to emission forward and back in the center-of-mass system. It should be noted that, because the incident particle is heavier than the target, all neutrons are emitted forward in the laboratory system, so that there are two "geometric" groups at all energies. Moreover, the whole conical beam contains, at different angles, all energies between the two 0° groups. Therefore, the reaction is not useful for obtaining mono-energetic neutrons. As a thick source, it has the limitation that the maximum and minimum energies separate relatively slowly. At an incident energy of 14 Mev, the maximum and minimum energies are 2.34 and 0.88 Mev, respectively, and at a 15-Mev incident energy are 3.03 and 0.68 Mev. Thus, the neutron energy spectrum produced by a 15-Mev accelerator would be somewhat limited.

The total neutron yield of the inverse lithium source was estimated by making a number of assumptions thought to be reasonable. First, a 15-μa lithium-7 beam was assumed to be incident on a pure hydrogen target.

Next, it was assumed that the distribution of neutrons for a given incident energy was uniform per unit solid angle in the cone of emission. On this basis, the yield per unit solid angle for an infinitely thick target, as a function of incident lithium ion energy was calculated as shown in Figure 9. The square sides at maximum angle result from the use of finite increments of the incident energy to compute the yields. For comparison, the yields of a $Li^7(p,n)Be^7$ target, of the same energy spread, are shown by horizontal dashed lines in which a 30-μa proton beam was assumed. It should be noted that in computing the total yield over the whole cone, a weighting factor proportioned to sin θ must be used. Hence, when an energy of 14 Mev is reached, the total yield of the $Li^7(p,n)Be^7$ reaction over the whole cone is comparable to that of the inverse reaction.

A final consideration is that of constructing the system. Two things are important for evaluating it. First, the existing heavy-ion accelerators give comparatively long bursts of ions, lasting a fraction of a microsecond. By comparison, a proton burst of less than one nanosecond can be produced. The second consideration is that no suitable proton target exists for the lithium beam. At these energies, the ions in the beam will be preponderantly triply ionized. This means greater energy dissipation in any target window than would result with protons. Thus, present technology would limit the beam to less than 5 μa, resulting in a yield less by a factor of three than that listed above. Any target except pure hydrogen would result in a great loss of yield due to the increased stopping power.

In light of these considerations, it appears that the construction of a heavy-ion accelerator for the purpose of making a neutron source based on the inverse lithium reaction would not be worthwhile. However, if someone especially needed a self-collimated neutron beam, or had a heavy-ion accelerator available, the scheme might be worthwhile trying.

3. Computer-controlled Multiparameter Data Accumulation and Processing System

The recently purchased 160-A computer has been placed into operation and has performed in an "on line" mode without failure for a period of five weeks. Measurements are being made of the mass distribution of fission fragements from U^{235} as a function of incident neutron energy and also for the spontaneous fission of Cf^{252}. The present experimental setup utilizes two solid-state detector systems, two analog to digital converters, and appropriate multiplexing circuitry for the sequencing of information into the computer. Each of the fragment pulses is digitalized to 6 binary places and the corresponding 12 binary bits from both analog to digital converters specify one address in one-half of the 160-A memory arranged in a 64 x 64 matrix. Each time an address is specified by a qualified event, a single count is added to the contents of that address. After an appropriate number of counts have been accumulated, the computer transfers it to an

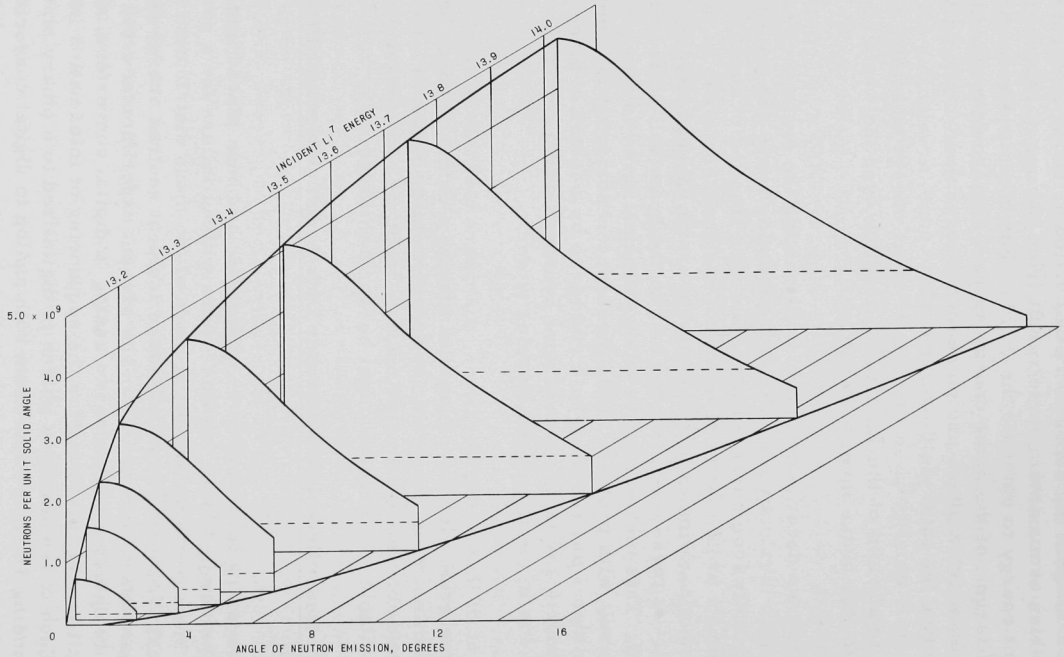

Figure 9. Neutron Yields from the Inverse Lithium Reaction. Yields of the $Li^7(p,n)Be^7$ reaction are shown for comparison with dashed lines. See text for assumptions made in computing the yields.

output routine in which the matrix is punched out on paper tape and also typed out for immediate visual inspection.

Although the final data-processing routines have not been programmed yet, the two fission peaks seem to be quite well separated. The rate at which the computer can store information in this mode of operation is about 53 μsec per fission fragment pair. This period is independent of the analog to digital conversion time, and it does not necessarily add to the dead time, since both operations can proceed simultaneously.

A computer-controlled CRT monitoring system will be in operation within four weeks. Immediate plans also call for two faster analog to digital converters with a more versatile multiplexing circuitry to accommodate more modes of data accumulation.

4. High Conversion Critical Experiment - ZPR-VII

The program of measurements planned for the core assembly composed of 3 w/o enriched uranium, stainless steel-clad, Hi-C fuel pins in a 1.24-cm square pitch pattern has been completed, unless subsequent analysis of the experimental data reveals an inconsistency that will require additional measurements for resolution. While the accumulated data are being processed, the bucklings for some less compact lattices will be established to provide an overlap with results available from work performed elsewhere on moderately enriched uranium-light-water lattices.

To make possible a precise determination of the buckling for the 1.24-cm square lattice, many axial and radial flux patterns have been measured, with bare and cadmium-covered gold, indium, dysprosium, enriched uranium, and depleted uranium. The bucklings derived from the conventional Cofit (cosine fits) and Jofit (Jo fits) treatment will be compared with the more elaborate analysis described in ANL-6658 (Progress Report for November 1962, p. 36) to determine the adequacy of the more simple method. The Cofit treatment of the several axial traverses has given values for B_z having a spread of about 2%, with some evidence of a dependence on the type of foil material used.

The data required for the determination of the initial conversion ratio, the fast effect, and the resonance escape probability have been acquired. Cadmium ratio measurements have been made with foils of gold, indium, dysprosium, Lu^{175}, Lu^{176}, manganese, and copper in the fuel pins, and with gold, indium, manganese, and copper in the water between the fuel pins. These two sets of measurements will provide spectral information and permit some sort of estimate of the flux depression within the fuel pins in the region of the U^{238} resonances.

5. Theoretical Physics

Doppler Effect Studies - Cross-section Evaluation. An IBM-704 program, RE-270, is now available for calculating resonance integrals for isolated resonances in the narrow resonance approximation, taking account of the statistical distribution of neutrons and fission widths. This program has been applied to the calculation of Pu^{239} cross sections as a function of temperature, σ_p(reactor scattering cross section in barns per Pu atom), and μ, the assumed number of channels per fission. The following assumptions were made: $\langle \Gamma_f \rangle = 0.099$ ev; $\Gamma_\gamma = 0.039$ ev; $\langle \Gamma_n^0 \rangle / D = 1.0 \times 10^{-4}$; and level spacing D = 11.6 ev for J = 0 and 3.86 ev for J = 1. Some results are given in Table VII. The sharp change in capture-to-fission ratio with assumed μ should be noted. Work of Bollinger[1] and of Vogt[2] indicates that μ probably equals 1 or 2. The data of Table VII do not include a p-wave contribution of about 0.3 b to σ_f and 0.15 b to σ_γ at 6.50 kev, and a contribution of about 0.2 b to σ_f and 0.1 b to σ_f at 2.25 kev. Negligible temperature variation is expected for the p-wave contribution.

Table VII. Isolated Level Calculations for Pu^{239} Fission and Capture

s-wave only

Neutron Energy, kev	$\mu = 1, \sigma_p = 300$					$\mu = 2, \sigma_p = 300$					$\mu = 3, \sigma_p = 300$				
	300°K		2500°K		$(\sigma\gamma/\sigma_f)$ 2500°K	300°K		2500°K		$(\sigma\gamma/\sigma_f)$ 2500°K	300°K		2500°K		$(\sigma\gamma/\sigma_f)$ 2500°K
	σ_f	$\sigma\gamma$	σ_f	$\sigma\gamma$		σ_f	$\sigma\gamma$	σ_f	$\sigma\gamma$		σ_f	$\sigma\gamma$	σ_f	$\sigma\gamma$	
6.50	1.535	1.093	1.556	1.108	0.712	1.767	0.994	1.791	1.007	0.560	1.870	0.949	1.896	0.962	0.507
2.25	2.89	2.21	2.99	2.29	0.765	3.35	1.97	3.48	2.05	0.590	3.56	1.87	3.69	1.94	0.525
0.61	5.62	4.58	6.15	5.09	0.827	6.54	4.00	7.19	4.44	0.619	6.94	3.74	7.65	4.15	0.543
0.18	9.08	7.47	10.63	9.22	0.865	10.50	6.46	12.42	7.90	0.635	11.13	6.01	13.22	7.31	0.553
0.061	12.75	10.00	15.19	13.21	0.870	14.59	8.70	17.65	11.22	0.636	15.39	8.12	18.73	10.36	0.553

Neutron Energy, kev	$\mu = 2, \sigma_p = 200$				$\mu = 2, \sigma_p = 400$			
	300°K		2500°K		300°K		2500°K	
	σ_f	$\sigma\gamma$	σ_f	$\sigma\gamma$	σ_f	$\sigma\gamma$	σ_f	$\sigma\gamma$
6.50	1.748	0.983	1.783	1.003	1.776	0.999	1.795	1.009
2.25	3.26	1.92	3.44	2.02	3.40	2.00	3.50	2.06
0.61	6.10	3.72	6.93	4.28	6.79	4.16	7.34	4.53
0.18	9.34	5.69	11.42	7.24	11.28	6.98	13.04	8.30
0.061	12.57	7.38	15.46	9.76	16.07	9.68	19.15	12.24

The effect of resonance overlap on the Doppler effect is being studied by evaluating resonance integrals for pairs of overlapping resonances. A number of such integrals have been calculated. The results have not yet been analyzed.

---

[1] Bollinger, J. M., Experimental Tests of Fission and Reaction Theory for Slow Neutrons, Proceedings of the International Conference on Neutron Interactions with Nuclei, Columbia University (1957).

[2] Vogt, E., Phys. Rev. 118, 724 (1960).

B. Reactor Components Development

1. Development of Viewing Systems

Studies of the electrical properties of glass have continued to achieve better understanding of the radiation-induced coloration of glass and the phenomena of radiation-induced voltage buildup in glass which has resulted in fracture in a few shielding windows (see Progress Report for September 1962, ANL-6619, p. 40). It has been observed that charge displacement occurs when an irradiated glass sample is heated between electrodes in the absence of an externally applied voltage, but with a thermal gradient across the sample. Recent measurements have been made with a gradient as low as 0.6°C/mm, extending previous measurements with a gradient ranging from 40°C/mm down to 2°C/mm. The charge displaced has continued to decrease nearly proportionally to the thermal gradient.

When a voltage was applied to the sample with a polarity tending to counterbalance the charge displacement, it was found that about 2000 v was required. Also, it has been reported previously that a reversal of the temperature gradient resulted in a complete reversal of the charge displaced. Thus, it appears that if an electrical field is induced by irradiation in the glass, the charge migration produced by this field is small in comparison to the charge migration induced by the thermal gradient.

In general, it is observed that, when the irradiated sample is heated, the rate at which the charge migration occurs is not a smooth function. Instead, several current maxima are observed at various temperatures, with the one occurring at the highest temperature always being of the opposite polarity. It has been reported that the addition of a small amount of cerium to the glass considerably altered both the magnitude and temperature location of these current maxima. Currently, a thermoluminescent peak has been observed to coincide with a charge-migration peak occurring at low temperatures. Both of these observations tend to support the postulate that a relationship, not yet understood, exists between the induced coloration and the charge migration induced by heating the sample in a thermal gradient.

2. Development of Manipulators for Handling Radioactive Materials

The electrically connected master-slave manipulator Mark IV will have a load capacity of 50 lb and will be designed to be mounted either on an overhead carriage system or on a vehicular system. The arm and overall configuration will be designed to achieve good dexterity, operating ease, and remote repairability. A pair of similar arms should be capable of repairing a manipulator by replacement of subassemblies. The design will also emphasize the reliability of all system components and the moderate cost of fabrication. The "vertical" motion of the arm will be obtained with telescoping members, rather than the elbow motion used on the Model 3 Electric Master-Slave Manipulator in order to reduce the operating space within the cave and to enable the operator to work closer to the window.

The slave servo drive units have been designed to obtain a shape which will give a reasonably compact assembly of the units. Each unit consists of 4 servo motors, three-stage spur gearing to give a reduction of 40, a position transducer, and a brake. Since fourteen of these units are required for a complete arm, considerable attention was given to cost reduction.

The control system will use separate power amplifiers for the master and slave arms. This simplifies the means of obtaining force amplification from the master to the slave arm and makes it possible to use the servo drive units to counterbalance the arm partially. A 200-w all-solid-state power amplifier has been developed and tested previously (see Progress Report for June 1962, ANL-6580, pp. 39-40). Investigation of various position transducers has been made which would reduce noise pick-up without requiring shielding of the leads. A resolver has been found which may be satisfactory, and a low-resistance potentiometer shows promise.

A carriage and turret unit has been built which is suitable for supporting a pair of electric master-slaves on an overhead rail system. All four support wheels are driven from a motor-gear-box unit which is remotely replaceable. These support wheels can be easily retracted so that the entire unit can be lowered between the rails.

C. Heat Engineering

1. Heat Transfer Analysis for EBWR Shipping Cask

A study of the heat transfer problems present in the design of shipping containers for EBWR spent fuel is in progress. The container is to be suitable for the existing EBWR plate and spike assemblies and for the plutonium-fueled assemblies required for future EBWR operations. The design will, of course, meet the AEC regulatory requirements for this equipment. Both water-cooled and dry casks will be considered.

2. Studies of Boiling Metals

A second electron-heating model was constructed for use in the boiling metal studies program. This model consists of a 0.020-in. thoriated tungsten cathode surrounded by a $\frac{3}{8}$-in.-OD, Type 316 stainless steel anode of 0.035-in. wall thickness. The 4-in.-long unit will be operated with a 4600-v, 1-amp power supply. When operating at peak power, an emission current of 0.618 amp/cm^2 from the cathode will produce a heat flux of 0.480×10^6 Btu/(hr)(ft^2) on the outside anode surface.

The vacuum system for use with the equipment is being assembled. It is planned to operate the electron-heating models in a vacuum between 10^{-5} and 10^{-6} mm Hg.

D. Chemical Separations

1. Chemical-Metallurgical Process Studies

a. Chemistry of Liquid Metals. In phase studies of the uranium-zinc system, it has been found that the delta phase (U_2Zn_{17}) cannot be formed below 550°C and, once formed at a higher temperature, will not decompose to the epsilon phase and uranium when held below 550°C. To demonstrate that minor amounts of impurities present in previous preparations of the delta phase were not responsible for this apparent anomaly, an experiment was performed in which high-purity uranium and zinc were used for the preparation of the delta phase. The alloy was annealed for 10 days at 400°C. No evidence of the epsilon phase was found.

Provisional values for the enthalpy and entropy of formation of the plutonium-zinc intermetallic phase $PuZn_{8.5}$ have been computed from the emf of galvanic cells. Mean values obtained from two cells believed to be the most reliable (see Progress Reports, August and November 1962, ANL-6610, p. 58, and ANL-6658, p. 54) are $\Delta Hf° = -74.2 \pm 0.3$ kcal/mole and $\Delta Sf° = -45.4 \pm 0.4$ cal/(deg)(mole).

The yttrium-zinc system is being studied by means of the recording effusion balance. Effusion isotherms at 520°C have indicated the existence of the following phases: YZn_{12}, Y_2Zn_{17}, $YZn_{4.5}$, YZn_3, and YZn_2. An additional phase was indicated by a slight inflection in the curve between Y_2Zn_{17} and $YZn_{4.5}$. The existence of phases of lower atomic ratios than 2 Zn:1 Y has not yet been determined. X-ray studies have confirmed the compounds Y_2Zn_{17} (structure of epsilon U_2Zn_{17}) and YZn_{12} (structure of $ThMn_{12}$). The phases $YZn_{4.5}$ and YZn_2 revealed complex patterns which require further study for their interpretation. These results may be compared with the phase diagram reported by Chiotti,[3] which shows the following phases: YZn_{11}, Y_2Zn_{17}, YZn_5, YZn_4, YZn_3, YZn_2, and YZn.

b. Conversion of Uranium Hexafluoride to High-density Uranium Dioxide. The preparation of coarse (+14 mesh) dense uranium dioxide particles directly from uranium hexafluoride by the simultaneous reaction of hexafluoride with steam and hydrogen was studied further (see Progress Report, November 1962, ANL-6658, p. 53). Because the gas velocities required to fluidize dense particles of this size cannot be accommodated by the present installation, a gas impulse was superimposed on the inlet gas flow to achieve mixing of the bed in the reactor. The pulse frequency used was about 30 pulses per minute with pulse durations of $\frac{1}{4}$ to one second in length. Although adequate operation of the system could be maintained, this method of bed agitation produced low-density, friable uranium dioxide product. Material newly deposited on uranium dioxide particles showed poor

---

[3] Chiotti, P., Mason, I. T., and Gill, K. J., IS-500 (1961), p. M-22.

adherence. Attrition of the uranium dioxide particles in the reactor bed resulted in the collection of an overhead fines fraction which was almost equivalent to the total uranium dioxide produced. Hence, particle growth was negligible. On the basis of these results, further work on the preparation of uranium dioxide in this size range is being discontinued.

c. Preparation of Plutonium Carbides. Equipment for the preparation of plutonium carbides has been installed and is being tested. It provides a purified helium atmosphere in a glove box which contains apparatus for performing gas-solid reactions, gas-liquid metal reactions, reactions in liquid metal solutions, and retorting.

d. Preparation of Uranium Monosulfide. In the preparation of uranium monosulfide, finely divided uranium metal powder is contacted with the stoichiometric quantity of hydrogen sulfide at 500°C. The products of this reaction are then heated in vacuum at approximately 2000°C to produce the uranium monosulfide. The first products which were prepared on a 40-gm uranium scale proved to be contaminated with impurities, primarily oxygen. Reworking and modification of the apparatus has resulted in a reduction of the oxygen contamination to less than 0.1 w/o.

e. Reduction of Thorium Dioxide. Four additional laboratory-scale runs have been performed to demonstrate the reduction of thorium dioxide to the metal by zinc-magnesium solution in the presence of molten halide fluxes. In these runs, thorium oxide charges were used which would yield thorium metal concentrations of 6.5 or 9.1 weight percent in the final zinc-magnesium solution. Values for the reduction of thorium dioxide to metal were 97, 93, 99, and 98 percent; pouring yield values were 92, 92, 91, and 92 percent. Thorium material balances for pairs of consecutive runs were 97.5 percent and 99.5 percent. Arc-melted thorium buttons weighed 32 to 54 gm and contained about 0.05 w/o metallic impurities.

2. Fluidization and Fluoride Volatility Separations Processes

a. Fluoride Separations. Studies of processes for the separation of plutonium hexafluoride from uranium hexafluoride are being continued. The effect of radiation on the decomposition of plutonium hexafluoride is being studied to provide information which is of fundamental interest in the development of these processes. Additional data have been obtained on the gamma-radiation decomposition of plutonium hexafluoride to plutonium tetrafluoride and fluorine when irradiated alone or in the presence of krypton. The results of current and previously reported experiments (see Progress Report, September 1962, ANL-6619, p. 46) have been used to establish a G value* of 7.4 for the decomposition of plutonium hexafluoride alone at 80 to 100 mm Hg pressure (25°C) by gamma radiation (~0.75 Mev) up to an absorbed dose of 3.73×10^{21} ev. Experiments on the gamma irradiation of plutonium hexafluoride samples (at 80 mm Hg pressure) containing

*Molecules decomposed per 100 ev of radiation.

krypton at one-half, one, and two atmospheres have resulted in G values of 2.9, 6.4, and 1.0, respectively. The absorbed energy doses for the three runs were 3.45×10^{21}, 2.65×10^{21}, and 8.85×10^{21}, respectively. The G values at one atmosphere and at two atmospheres are in general agreement with previously reported results. The G value for the run made with krypton at one-half atmosphere has not been substantiated. Additional experiments are planned.

The absorption spectrum of gaseous plutonium hexafluoride was determined in the ultraviolet, visible, and near infrared regions. The predominant peak in the ultraviolet is at 2090 Å with a molar extinction coefficient of 2670 l/(mole)(cm). Several peaks are evident in the visible region between 4100 and 5800 Å. The major peaks in the near infrared region are grouped in two bands, one at approximately 8000 Å and the second at approximately 10,000 Å.

The spectrum of plutonium hexafluoride in the region from 2000 to 4000 Å shows relatively strong absorption. In contrast, UF_6 shows very little absorption at wavelengths greater than 3200 Å in the ultraviolet region (see ANL-5254, p. 49). At 3400 Å, the ratio of molar extinction coefficients of gaseous PuF_6 and UF_6 is approximately 600. The difference in absorbancies of PuF_6 and UF_6 in the ultraviolet region may make it possible to use absorption spectrometry for inline process analysis.

The need for an analytical procedure for uranium hexafluoride and plutonium hexafluoride in mixtures of these compounds has also stimulated a study of the chemical reactions of carbon disulfide with uranium hexafluoride and plutonium hexafluoride. Uranium hexafluoride is found to react readily with dry carbon disulfide at room temperature. When excess uranium hexafluoride is used, the solid reaction product is U_2F_9. When excess carbon disulfide is used, the solid reaction product appears to be powdered uranium tetrafluoride. However, further analysis of the product is needed before positive identification can be made. When the reaction mixture is allowed to reach 100 to 200°C, the gaseous products formed are sulfur tetrafluoride (SF_4), sulfur hexafluoride (SF_6), carbon tetrafluoride (CF_4), bistrifluoromethyldisulfide [$(CF_3)_2S_2$], and possibly bistrifluoromethyltrisulfide [$(CF_3)_2S_3$]. When the reaction proceeds to completion at room temperature, the main gaseous products are $(CF_3)_2S_2$ and $(CF_3)_2S_3$ with a trace of SF_4.

Plutonium hexafluoride also reacts very readily with carbon disulfide at room temperature. The solid product of the reaction is finely powdered plutonium tetrafluoride (PuF_4). The gaseous products are SF_4, SF_6, and CF_4.

The reaction between uranium hexafluoride vapor and hydrogen sulfide gas has also been investigated. The reaction takes place readily at

25°C to produce uranium tetrafluoride, sulfur tetrafluoride, and hydrogen fluoride. When the reaction temperature is 100 to 500°C, free sulfur and sulfur hexafluoride are formed in addition to the above products.

An experiment to obtain information about the reaction of plutonium hexafluoride with calcium fluoride was made. A 0.4-gm sample of powdered, prefluorinated calcium fluoride was contacted for one hour at room temperature with about an equal weight of plutonium hexafluoride. Both solid and gaseous plutonium hexafluoride were in contact with the calcium fluoride. After one hour, the plutonium hexafluoride was removed by vacuum distillation (pressure about 2.5×10^{-4} mm) at room temperature. An analysis of the calcium fluoride for plutonium indicated that approximately 0.7 percent (3 mg) of the initial plutonium hexafluoride was present. Calculations based on these data would indicate that adsorption of plutonium hexafluoride on calcium fluoride could account for the retention of this amount of plutonium hexafluoride. The 3 mg of plutonium hexafluoride could be adsorbed on 17 percent of the available surface area of the calcium fluoride.* Workers at Oak Ridge have postulated that plutonium hexafluoride forms a stable complex with calcium fluoride. Therefore, it is possible that, in the ANL experiment, a compound may have formed which decomposed at the low pressures ($\sim 2.5 \times 10^{-4}$ mm) to which the system was subjected. Further experimental work will be necessary to characterize the mechanism in this reaction.

b. Plutonium Pilot Plant Facility. Work on the installation of the engineering-scale plutonium-handling facility is continuing (see Progress Report, July 1962, ANL-6597, p. 43). The installation of the two alpha enclosures has been completed. Design of ventilation for the room and alpha enclosures and of instrument connections from the panel board to the alpha enclosures is being detailed. Most of the equipment and accessories needed for the study of the fluorination of uranium-plutonium oxide pellets has been fabricated and delivered. Equipment for the separation of uranium from plutonium is being designed.

The efficiency and capacity of the uranium hexafluoride condenser were determined prior to the installation of the condenser in the alpha enclosure. The capacity tests were made at the flow rates proposed for the pilot-plant facility, i.e., a total gas flow of one cfm nitrogen and about 3 lb UF_6/hr. Collection efficiencies greater than 99 percent were obtained for capacities up to about 50 lb UF_6.

c. Separation of Uranium from Zirconium Alloy Fuels.

(i) Studies of the Chlorination and Fluorination Steps. Bench-scale fluid-bed studies on the chlorination-fluorination scheme for reprocessing highly enriched uranium-zirconium alloy fuels are continuing (see

*A sample of calcium fluoride dried at 120°C overnight in a helium atmosphere showed a specific surface area of 12.7 sq m/g.

Progress Report, November 1962, ANL-6658, p. 52). In the present study, the chlorination-fluorination reaction sequence consisted of hydrochlorination followed by reaction with fluorine. Multiple batching of uranium-zirconium alloy chips during hydrochlorination was again utilized (see Progress Report, October 1962, ANL-6635, p. 45). Three batches of alloy chips were charged during the hydrochlorination step, each charge consisting of about 240 gm of 5 w/o uranium-zirconium chips ($\frac{1}{8}$ to $\frac{1}{4}$ in. in size). The run cycle time was 28.5 hr. The run included 20.5 hr. of reaction with hydrogen chloride at 400°C (each batch was charged successively and reacted with hydrogen chloride for 4.3, 3.9, and 12.3 hr, respectively), 2 hr of reaction with fluorine at 350°C, followed by 6 hr of reaction with fluorine at 500°C. In the hydrochlorination step, the second and third 240-gm batches of alloy chips were added after a major fraction of each of the previous charges was reacted and while high reaction rates and high efficiences of reactant utilization were still being maintained. Data from the hydrochlorination step indicate that 70 percent of the first 240 gm of alloy chips had reacted before the second 240-gm charge was added and that about 80 percent of the alloy chips from the first two charges had reacted before the third 240-gm charge was added. Alloy reaction rates up to 90 gm/hr were achieved with an average value of 70 gm/hr during the steady-state portion of the run. This may be compared with the reaction rate of 50 gm/hr reported previously (see Progress Report, October 1962, ANL-6635, p. 46). The increase in the alloy reaction rate is due to the higher concentrations of reactants that were used in the present study. The use of higher concentrations was made possible by the introduction of a more efficient cooling system for the fluid-bed reactor.

(ii) Pilot Plant for Processing Enriched Uranium-Zircaloy Alloy Fuels. The major items of process equipment for the pilot plant to demonstrate the reprocessing of enriched uranium-zirconium type of fuels have been installed (see Progress Report, August 1962, ANL-6610, p. 58). These include the primary reactor and hydrolysis column, down-flow filter, fluorine disposal columns, a condenser, and a diaphragm pump for gas recycle. Electrical work is now in progress.

3. Calorimetry

The heat of formation of tetrafluoromethane is being investigated. An apparently satisfactory analytical method is available for determining the small amount of C_2F_6 (0.1 to 1 percent) side product formed in the combustion of carbon in fluorine. Presently, exploratory work is being directed toward finding satisfactory ignition techniques.

In an investigation of the heat of formation of tantalum pentafluoride, two series of combustions of tantalum in fluorine have been completed. Analysis of combustion products is in progress.

IV. PLUTONIUM RECYCLE REACTOR PROGRAM

Calculations have been made for the three-zone core configuration to study the effect of using a dispersed burnable poison in the enriched uranium shim (middle) zone, and for length of irradiation when the central region is fueled with plutonium and the outer region is fueled with natural uranium. The calculations were based upon an initial uranium enrichment of 6% and a ratio of 3000:1 of enriched uranium to B^{10}, the dispersed poison, and indicate that it will undergo an irradiation period corresponding to approximately that possible with an unpoisoned initial shim zone and its first replacement. The poisoned configuration also has the advantage of flattening the power distribution in the core.

A two-dimensional calculation has been made for the three-zone poisoned system. These results will be used as the starting point for calculating accurately the power-void prediction for the system at 60 Mw.

The influence of void on material cross sections has been examined, and correction factors have been generated for use in the burnup calculations.

V. ADVANCED SYSTEMS RESEARCH AND DEVELOPMENT

A. Argonne Advanced Research Reactor (AARR)

1. Critical Experiment

Specifications for the uranium foil which is to serve as fuel in the critical core have been defined and are being drawn up in final form for procurement.

An auxiliary readout device for the new compact rod drives has been constructed and tested. The response of the device has been found to be satisfactory and reliable. A study directed toward simplification of the final production design is in progress.

Cell modification, piping revisions, and fabrication of core components have been initiated.

2. Production of Higher Fluxes in AARR

The heat transfer study of proposed AARR cores reported earlier (Progress Report for October 1962, ANL-6635, p. 53) was extended to assess the feasibility of producing higher neutron fluxes than originally contemplated. An ultimate goal of 1×10^{16} n/(cm^2)(sec) thermal in the internal thermal column was set. This would correspond to about 2×10^{15} n/(cm^2)(sec) in the experimental beam tubes.

Both the Case 1 and Cast 2 cores* previously investigated were studied. It was calculated that, with the Case 1 core, a reactor power level of 239 Mw was required to produce the desired fluxes, whereas 204 Mw was required for Case 2. Operation with local boiling was assumed, and corresponding values of system pressure and core coolant velocity were determined such as to allow a 25% power overshoot before inception of bulk boiling.

For the Case 1 core, the study showed that at a system pressure of 750 psi and a core coolant velocity of 45 fps, the reactor could operate at the 240-Mw level to produce the desired thermal neutron flux of 10^{16} n/(cm^2)(sec). Thus, the AARR facility could be provided with the potential for ultimately reaching a flux of 10^{16} n/(cm^2)(sec) by the relatively simple expedient of: (a) increasing the primary system design pressure from its present value of 500 psi to 750 psi; (b) increasing the developed head requirement of the primary pumps by a small amount;

*The Case 1 core has fuel plate thicknesses and coolant channel spacings each equal to 0.040 in., whereas the Case 2 core has 0.050-in.-thick fuel plates and 0.030-in. channel spacings. In both cases the total core volume is 77 liters.

and (c) designing for ease of later installation of an additional 140 Mw of primary heat-exchanger capacity and corresponding secondary heat-dissipation equipment.

For the Case 2 core, although a lower power level is needed for a flux of 10^{16} n/(cm^2)(sec), higher system pressures and velocities are needed because the narrower coolant channels make this core inherently less stable, and costs are higher.

The unique feature of AARR which permits consideration of such an eventual up-rating is the stainless steel core. With stainless steel, higher core coolant velocities and higher fuel temperatures are feasible than with aluminum. Moreover, the elimination of the xenon problem by operation with an epithermal energy spectrum, and the inherently longer core life, minimize problems which would be virtually insurmountable with aluminum cores. It is also feasible that the development of production techniques for UO_2-stainless steel matrices having higher than the present maximum UO_2 content of 37 wt-% could result in cores having as long a life as that now expected for the present reference core (75 to 90 days).

B. Underseas Application of Nuclear Power

A new set of calculations are being performed to establish the design parameters for the 2000-hp pressurized water reactor system to be used in a submergible research vessel. A reduction in the lifetime requirement from 2 to 1 yr prompted the new calculations. The new calculations are based upon a smaller core, ~12 in. in diameter by 12 in. high versus one that was ~20 in. in diameter by 22 in. high. The same heat output is achieved by increasing the coolant flow rate. The criticality calculations are being processed to establish the fuel loadings for various coolant volume fractions. When the core parameters are determined, the balance of the components in the primary system will be redesigned to provide for the new conditions.

VI. NUCLEAR SAFETY

A. Thermal Reactor Safety Studies

1. Metal Oxidation and Ignition Studies

An experimental method has been developed for the study of the oxidation of uranium by air at temperatures above 700°C. In this method, one-cm cubes of uranium are supported on thermocouples and heated by an external induction coil. Mixtures of air and argon are passed over the heated sample, and the depletion of oxygen and nitrogen in the effluent gas is measured continuously by a mass spectrometer. The results of a preliminary experiment at 700°C indicate that the oxidation rate of uranium corresponds to a linear rate law.

Ignition temperature of 0.5-cm cubes of plutonium and plutonium alloys have been determined by the burning-curve method in oxygen and in air. In this method, the sample is heated at a uniform rate (usually 10 deg/min) in a flowing atmosphere of the oxidant. As the rate of reaction increases, the sample self-heats and finally ignites. The temperature at which the sample ignites is determined by a graphical method (see Chemical Engineering Division Summary Report for April, May, June 1962, ANL-6569, p. 136). Plutonium samples with a specific area of approximately 0.7 sq cm/g were found to ignite at 500°C in oxygen and at 510°C in air. The addition of a nominal two percent of an additive to the plutonium was found to increase the ignition temperature only slightly in the cases of aluminum, copper, and silicon; the greatest increase (60°C) in ignition temperature was caused by the addition of aluminum. Additions of magnesium, chromium, iron, zinc, cerium, and uranium had a negligible effect on the ignition temperature of plutonium. Plutonium alloys with manganese, cobalt, or nickel ignited at temperatures 30 to 40°C below the ignition temperature of plutonium.

2. Metal-Water Studies

Study of the reaction of stainless steel with water by the condenser-discharge method was continued. In this method, metal wires are rapidly melted and dispersed in a water-filled cell by a surge current from a bank of condensers. The energy input to the wire is used to calculate the initial reaction temperature. The extent of reaction in the current series of experiments was determined by the measurement of the quantity of hydrogen evolved, based on the formation of the following oxides: Cr_2O_3, NiO, and FeO. The experiments were performed using 30-mil wires of stainless steel-316 (18 percent chromium, 12 percent nickel, 2 percent molybdenum, remainder iron) in water at 315°C. The percent of metal that reacted with water varied with the initial temperature of the metal. Results of six runs were as follows:

Calculated Initial Temperature of Metal (°C)	Percent Reaction
2200	10.1
2300	16.5
2600	17.8
2800	21.8
2900	31.6
3500	34.2

The extent of reaction obtained in this series of runs made at 315°C (1500 psia) was nearly identical to the extent of reaction observed in previous experiments carried out in water at 100°C (15 psia) and 200°C (225 psia). In studies of the zirconium-water reaction,[5] the extent of the reaction was also found to be independent of the water temperature and vapor pressure. These findings suggest that the kinetics of the oxidation process for both stainless steel and zirconium are independent of pressure over a wide range.

In-pile studies of metal-water reactions in the TREAT facility were continued. Four additional experiments were carried out with 60-mil-thick, 0.5-in. by 1.4-in. plates. These plates contained a 20-mil-thick core of aluminum-23 weight percent uranium (fully enriched) alloy which was clad in 20-mil-thick 2S aluminum. The plates were subjected to nuclear bursts which supplied energies of 527, 577, 731, and 794 cal/gm of plate. The plates reacted with water to the extent of 11.0, 11.0, 13.6, and 36.9 percent, respectively. The amounts of xenon-133 released to the gas in the experimental assemblies were found to be 33.5, 37.7, 35.4, and 49.0 percent, respectively, of the xenon-133 produced by fission. These results may be compared with results obtained in previous studies of the same system (see Progress Report, November 1962, ANL-6658, p. 68).

B. Fast Reactor Safety Studies

Experiments are being performed with TREAT to study the characteristics and causes of failure of fast reactor fuel elements, and to survey the effective mechanisms influencing fuel movement.

1. Transient Behavior of Pre-irradiated EBR-II Fuel Elements

In Series XXXV, four pre-irradiated EBR-II fuel elements were assembled remotely and exposed to transients in TREAT in dry opaque test capsules. The test elements were stainless steel-clad, sodium-bonded

[5] L. Baker, Jr. and L. C. Just, Studies of Metal-Water Reactions at High Temperatures. III. Experimental and Theoretical Studies of the Zirconium-Water Reaction, ANL-6548 (May 1962).

EBR-II pins, irradiated to an estimated burnup of approximately 2%, and annealed in a furnace for 5 hr at 550°C after irradiation. The results of the transient tests are shown in Table VIII.

Table VIII. Test Results of Series XXXV (Pre-irradiated EBR-II) Fuel Elements

Sample	Maximum Temperature (°C)	Condition after Test
1	820	Warped; no penetration; fuel diameter increased 0.004 in.
2	870	Warped; no penetration; fuel diameter increased 0.006 in.
3	960	Penetration; non-violent failure with fuel ejected through hole near bottom of element.
4	1060	Element parted at center, ~5 in. in top section, with signs of melting. Fuel ejected from bottom section in moderately violent failure.

It should be noted that the increase in diameter of specimens 1 and 2 is not necessarily the result of the transient test. This fuel expansion may have occurred during the irradiation and subsequent furnace heating. However, such a volume increase is typical of that observed for steady-state irradiations, to about 1% burnup, with maximum fuel temperatures of 540 to 620°C. The actual value of percentage burnup in the test elements that did not fail will be checked by burnup analysis of the fuel pin specimens.

2. Integral (Small) Sodium Loop Calibration

A small integral sodium loop was loaded with an unbonded 4.1% EBR-II prototype fuel element equipped with U^{25} foils and prepared for shipment to TREAT. The loop was mechanically complete, but contained no sodium.

The purpose for the exposure of the loop in TREAT is to obtain low power calibration data which will indicate the magnitude of flux to be expected at the test element during a transient.

3. Liquid Metal Pressure Instrumentation Development

A number of static calibration high-temperature proof tests were completed on two prototype pressure transducer standoff assemblies previously described (Progress Report for August 1962, ANL-6610, p. 68).

The results of the tests indicate that diaphragm-type pressure transducers can be used with liquid sodium systems at elevated temperatures with good accuracy.

The pressure transducer standoff units were mounted on a 2-in. by 30-in. autoclave filled with sodium. Each transducer body and mounting was enclosed in a thin-walled steel jacket through which dried filtered air at room temperature was passed as a coolant. The maximum pressure of cooling air applied to the transducer jackets was 10 psig. Static calibrations of the transducers were made at 150°C, 325°C, and 500°C.

At 500°C, the transducers in the standoff assemblies suffered a further decrease in full-range sensitivity of 2.5% maximum, with a total decrease of 5% from the prefabricated full-range sensitivity. The temperature-dependent decrease in sensitivity is in close agreement with the sensitivity decrease calculated from the manufacturer's specifications given for each transducer. No departure from the pre-fabrication linearity of pressure-versus-millivolt calibration could be detected in either transducer over the full range of temperature during thermal cycling and subsequent tests.

Further tests will be undertaken to evaluate the frequency response of the transducer standoff assembly, and the principle of design will be applied to other sodium-filled or high-temperature pressurized systems.

4. Installation of Sodium Loop in TREAT

Connection of wiring between the switchgear and stepdown transformer used to supply power for the loop heaters was completed. Installation of wiring between the electromagnetic pump rectifier and the instrument panels was also completed.

Five cylinder-operated valves for the loop were tested for leakage and proper actuation. Two of the valves leaked around the bellows seal assembly and one did not actuate properly. These valves will be returned to the manufacturer for repair.

The first of two resistance-type probes designed and built to record the levels in the loop storage and dump tanks was thermally cycled in NaK between room temperature and 400°C for one week. Operation was found to be satisfactory at all temperatures. Assembly of the second unit was completed, and it will be tested in NaK next month.

VII. PUBLICATIONS

Papers

STUDIES OF METAL-WATER REACTIONS BY THE EXPLODING WIRE TECHNIQUE

L. Baker, Jr, and R. Warchal

Exploding Wires, Vol. 2, Plenum Press, New York, 1962 pp. 207-233.

FISSION GAS RELEASE AND SWELLING DURING HEATING OF IRRADIATED EBR-II TYPE FUEL

N. R. Chellew, and R. K Steunenberg

Nuclear Sci. and Eng. 14 (1), 1 (1962)

THE APPLICATION OF OXYGEN- AND FLUORINE-BOMB CALORIMETRY TO NUCLEAR MATERIALS

H. M. Feder, D. R. Fredrickson, E. Greenberg, W. N. Hubbard, R. L. Nuttall, E. Rudzitis, J.L. Settle, and S. S. Wise

Thermodynamics of Nuclear Materials, International Atomic Energy Agency, Vienna, 1962. pp. 155-162.

PLUTONIUM HEXAFLUORIDE THERMAL DECOMPOSITION RATES

J. Fischer, L. E. Trevorrow, G. J. Vogel, and W. A. Shinn

I&EC Process Design and Development 1, 47-51 (1962).

THERMODYNAMICS OF THE BINARY SYSTEMS OF URANIUM WITH Zn, Cd, Ga, In, Tl, Sn AND Pb

I. Johnson, and H. M. Feder

Thermodynamics of Nuclear Materials, International Atomic Energy Agency, Vienna, 1962. pp. 319-329.

CERTIFICATION OF ALGORITHM 94 COMBINATION (J. Kurtzburg, Comm. ACM, June 1962)

R. E. Grench

Comm. ACM, Vol. 5, No. 12, p. 606 (December, 1962).

CERTIFICATION OF ALGORITHM 118 MAGIC SQUARE (ODD ORDER) (D. M. Collison, Comm. ACM, August, 1962)

Henry C. Thacher, Jr.

Comm. ACM, Vol. 5, No. 12, p. 606 (December, 1962).

MAGNETIC PROPERTIES OF IRRADIATED SA-212B PRESSURE-VESSEL STEEL

N. Balai and R. J. K. Blöch

Paper presented at International Atomic Energy Agency Symposium on "Radiation Damage in Solids," Vienna, May, 1962. Proceedings of Symposium on "Radiation Damage in Solids," pp. 193-203 (1962), IAEA.

ANL REPORTS

ANL-6460 ROOM-TEMPERATURE LATTICE CONSTANTS OF ALPHA URANIUM-PLUTONIUM ALLOYS
A. F. Berndt.

ANL-6495 A STUDY OF URANIUM-FISSIUM ALLOYS CONTAINING TECHNETIUM
R. W. Bohl and M. V. Nevitt

ANL-6554 INSTRUMENTED TEMPERATURE-CONTROLLED CAPSULES FOR IRRADIATIONS IN THE CP-5 REACTOR
W. N. Beck and R. J. Fousek

ANL-6628 AUTOMATIC FOIL ACTIVITY COUNTING FACILITY AND DATA-REDUCTION PROGRAM
K. E. Plumlee and M. T. Wiggins

ANL-6633 CONTRIBUTION TO THE THEORY OF TWO-PHASE, ONE-COMPONENT CRITICAL FLOW
Hans K. Fauske